Proc. 24th International Spin Symposium (SPIN2021)
JPS Conf. Proc. **37**, 020123 (2022)
https://doi.org/10.7566/JPSCP.37.020123

Global fits of unpolarized TMDs at N^{3}LL accuracy

Matteo Cerutti[1,2], Alessandro Bacchetta[1,2], Valerio Bertone[3], Chiara Bissolotti[1,2,4], Giuseppe Bozzi[5,6], Fulvio Piacenza[1,2], Marco Radici[2], and Andrea Signori[1,2]
for the *MAP collaboration*

[1] *Physics Department, University of Pavia, via Bassi 6, I-27100 Pavia, Italy*
[2] *INFN, Section of Pavia, via Bassi 6, I-27100 Pavia, Italy*
[3] *IRFU, CEA, Université Paris-Saclay, F-91191 Gif-sur-Yvette, France*
[4] *HEP Division, Argonne National Laboratory, 9700 S. Cass Avenue, Lemont, IL-60439 USA*
[5] *Physics Department, U. of Cagliari, Cittadella Universitaria, I-09042 Monserrato (CA), Italy*
[6] *INFN, Section of Cagliari, Cittadella Universitaria, I-09042 Monserrato (CA), Italy*

E-mail: matteo.cerutti02@universitadipavia.it (speaker)

(Received Tuesday, Feb. 15th, 2022)

We review the recent progress on the extraction of unpolarized TMD PDFs and TMD FFs from global data sets of Semi-Inclusive Deep-Inelastic Scattering, Drell-Yan and Z boson production. In particular, we address the tension between the low-energy SIDIS data and the theory predictions, and explore the impact of the very precise LHC data on the fit results.

KEYWORDS: QCD, hadron structure, hadronization, transverse momentum distributions

Introduction. An accurate knowledge of the unpolarized transverse-momentum-dependent (TMD) parton distribution functions (PDFs) and fragmentation functions (FFs) is one of the most important goals for the hadron structure and hadronization physics programs. Understanding their structure with high precision allows one to unravel the (un)polarized three-dimensional structure of hadrons in momentum space and has a significant impact on high-energy physics too. Working in a non-perturbative QCD regime, we need to complement perturbation theory with techniques to access the structure of the TMD distributions (TMDs). Among the different approaches available (continuum methods, lattice field theory, etc.) we rely on fits of experimental data sets.

SIDIS cross section. In the limit where leptonic and hadronic masses can be neglected, the differential cross section for unpolarized semi-inclusive deep-inelastic scattering (SIDIS) at small transverse momentum [1, 3] reads:

$$\frac{d\sigma^{\text{SIDIS}}}{dx\,dz\,d|\boldsymbol{q}_T|\,dQ} = \frac{8\pi^2\,\alpha^2\,z^2\,|\boldsymbol{q}_T|}{x\,Q^3}\left[1+\left(1-\frac{Q^2}{xs}\right)^2\right]\mathcal{H}(Q,\mu)\,F_{UU,T}(x,z,\boldsymbol{q}_T^2,Q)\,, \tag{1}$$

where x, z are the light-cone fractions associated to the collinear momenta of the incoming and outgoing quarks, respectively [1]; q is the four momentum of the exchanged photon, whose transverse component in the frame where the incoming and outgoing hadrons are collinear is $\boldsymbol{q}_T$ and for which $Q^2 = -q^2 > 0$; α is the QED coupling constant, $\mathcal{H}$ is the hard function, and μ the renormalization scale. Since we are interested only in the small transverse momentum limit, in Eq. (1) we have neglected the contributions from fixed-order calculations at high $|\boldsymbol{q}_T|$ and the matching of these to TMD factorization.

The unpolarized SIDIS structure function $F_{UU,T}$ is defined as [1]:

$$F_{UU,T}(x,z,\boldsymbol{q}_T,Q) = \frac{x}{2\pi}\sum_a e_a^2\int_0^{+\infty} d|\boldsymbol{b}_T||\boldsymbol{b}_T|J_0(|\boldsymbol{b}_T||\boldsymbol{q}_T|)\tilde{f}_1^a(x,\boldsymbol{b}_T^2;Q,Q^2)\,\tilde{D}_1^{a\to h}(z,\boldsymbol{b}_T^2;Q,Q^2) \tag{2}$$

where the sum runs over quarks and antiquarks a. The $\tilde{f}_1^a(x, \boldsymbol{b}_T^2, Q, Q^2)$ and $\tilde{D}_1^{a\to h}(z, \boldsymbol{b}_T^2, Q, Q^2)$ are, respectively, the Fourier transforms of the unpolarized TMD PDF for a quark a in a proton, $f_1^a(x, \boldsymbol{k}_\perp^2; Q, Q^2)$, and the TMD FF for a quark with flavor a fragmenting into a hadron with flavor h, $D_1^{a\to h}(z, z^2\boldsymbol{p}_\perp^2; Q, Q^2)$. The variable $\boldsymbol{b}_T$ is conjugated via Fourier transform to the transverse momentum $\boldsymbol{q}_T$ (and to the partonic transverse momenta $\boldsymbol{k}_\perp$ and $\boldsymbol{p}_\perp$, such that $\boldsymbol{q}_T = \boldsymbol{p}_\perp - \boldsymbol{k}_\perp$).

The observable provided by the Hermes and Compass collaborations is the multiplicity, namely the ratio of the one-hadron inclusive cross section over the fully inclusive one, as a function of the transverse momentum of the hadron $\boldsymbol{P}_{hT}$:

$$M(x, z, |\boldsymbol{P}_{hT}|, Q) \doteq \frac{d\sigma^{\rm SIDIS}}{dx\, dz\, d|\boldsymbol{P}_{hT}|\, dQ} \Big/ \frac{d\sigma^{\rm DIS}}{dx\, dQ}, \tag{3}$$

where $\boldsymbol{P}_{hT}$ is the transverse momentum of the observed hadron in the Breit frame, which is related to $\boldsymbol{q}_T$ as [2]:

$$\boldsymbol{q}_T = -\boldsymbol{P}_{hT}/z\,. \tag{4}$$

In Ref. [3] it was demonstrated that the $\boldsymbol{q}_T$-differential cross section in TMD factorization at the next-to-leading logarithmic accuracy (NLL) is able to correctly predict the normalization and the shape of the SIDIS multiplicities (apart from a y-dependent normalization factor associated to systematic experimental effects in the Compass analysis). At variance with Ref. [4], we find a significant tension between the experimental values for the SIDIS multiplicities and the calculations in TMD factorization beyond NLL. This tension has been observed independently by other groups and documented, for example, in Ref. [5]. In order to tackle this discrepancy, we use the method proposed in Ref. [6], which consists in introducing the following normalization factor:

$$\omega(x, z, Q) = \frac{d\sigma^{\rm SIDIS}}{dx\, dz\, dQ} \Big/ \int d|\boldsymbol{P}_{hT}|\, \frac{d\sigma^{\rm SIDIS}}{dx\, dz\, d|\boldsymbol{P}_{hT}|\, dQ}\,. \tag{5}$$

This factor accounts for the difference beyond NLL between the integral of the $\boldsymbol{P}_{hT}$-dependent SIDIS cross section and the collinear SIDIS cross section at the corresponding order in perturbation theory. Within the scope of our analysis, which is limited to the small transverse momentum region, the $\boldsymbol{P}_{hT}$-differential cross section is approximated with the TMD calculation. Beyond the NLL, the prefactor becomes different from 1 and, in general, does not depend on $\boldsymbol{P}_{hT}$ and any fit parameter. As a consequence, the theoretical expression for the multiplicity becomes:

$$M_\omega(x, z, |\boldsymbol{P}_{hT}|, Q) = \omega(x, z, Q)\, M(x, z, |\boldsymbol{P}_{hT}|, Q)\,. \tag{6}$$

Drell-Yan / Z-boson production cross section. The cross section for Drell-Yan and Z-boson production reads:

$$\frac{d\sigma^{\rm DY/Z}}{d|\boldsymbol{q}_T|\, dy\, dQ} = \frac{16\pi^2\alpha^2}{9Q^3}\, |\boldsymbol{q}_T|\, \mathcal{P}\, \mathcal{H}(Q,\mu)\, F_{UU}^1(x_1, x_2, |\boldsymbol{q}_T|, Q)\,, \tag{7}$$

where $\boldsymbol{q}_T$ is the transverse momentum of the intermediate boson, y is its rapidity ($y = \frac{1}{2}\ln\left(\frac{q_0+q_z}{q_0-q_z}\right)$), $\mathcal{P}$ is the phase space factor to account for potential cuts on the lepton kinematics [7], and $\mathcal{H}$ is the hard function of the process. At low transverse momentum $\boldsymbol{q}_T^2 \ll Q^2 = q^2 > 0$ the structure function can be expressed as a convolution over the partonic transverse momenta of two TMD PDFs:

$$F_{UU}^1(x_1, x_2, |\boldsymbol{q}_T|, Q) = \frac{x_1 x_2}{2\pi} \sum_a c_a(Q) \int_0^{+\infty} d|\boldsymbol{b}_T| |\boldsymbol{b}_T| J_0(|\boldsymbol{b}_T||\boldsymbol{q}_T|) \tilde{f}_1^a(x_1, \boldsymbol{b}_T^2; Q, Q^2)\, \tilde{f}_1^{\bar{a}}(x_2, \boldsymbol{b}_T^2; Q, Q^2)\,, \tag{8}$$

where $c_a(Q)$ are the electro-weak charges [7], $x_{1,2}$ are the longitudinal momentum fractions, which, in the small transverse momentum limit, take the values:

$$x_1 = \frac{Q}{\sqrt{s}} e^{y}, \qquad x_2 = \frac{Q}{\sqrt{s}} e^{-y}. \tag{9}$$

Transverse momentum distributions. The evolution of TMDs from the initial values of the renormalization and rapidity scales μ_i, ζ_i, to the final values μ_f, ζ_f, is given by

$$\tilde{f}_1^a(x, \boldsymbol{b}_T^2; \mu_f, \zeta_f) = \tilde{f}_1^a(x, \boldsymbol{b}_T^2; \mu_i, \zeta_i) \exp\left\{ \int_{\mu_i}^{\mu_f} \frac{d\mu}{\mu} \gamma_F\left[\alpha_s(\mu); \frac{\zeta}{\mu^2}\right]\right\} \left(\frac{\zeta_f}{\zeta_i}\right)^{-K(|\boldsymbol{b}_T|, \mu_i)}, \tag{10}$$

where α_s is the strong coupling constant and K is the Collins-Soper kernel [2]. The same structure holds for the TMD FF. The scale μ_i can be conveniently fixed as $\mu_b = 2e^{-\gamma_E}/|\boldsymbol{b}_T|$, and thus Eq. (10) is perturbatively meaningful only at low values of $|\boldsymbol{b}_T|$. The arbitrary matching to the non-perturbative regime at large $|\boldsymbol{b}_T|$ is accomplished by modifying the scale μ_b as $\mu_{b_{T*}} = 2e^{-\gamma_E}/b_{T*}$, with

$$b_{T*}(|\boldsymbol{b}_T|, b_{\min}, b_{\max}) = b_{\max} \left(\frac{1 - e^{-|\boldsymbol{b}_T|^4/b_{\max}^4}}{1 - e^{-|\boldsymbol{b}_T|^4/b_{\min}^4}}\right)^{1/4}, \tag{11}$$

where

$$b_{\max} = 2e^{-\gamma_E}\ \mathrm{GeV}^{-1} \approx 1.123\ \mathrm{GeV}^{-1}, \qquad b_{\min} = 2e^{-\gamma_E}/Q. \tag{12}$$

In this way, b_{T*} saturates to $b_{\max}$ at large $|\boldsymbol{b}_T|$, as suggested by the CSS formalism [2]. At small $|\boldsymbol{b}_T|$, the arbitrary matching to fixed-order collinear calculations is realized by saturating b_{T*} to $b_{\min}$. Accordingly, in the limit $|\boldsymbol{b}_T| \to 0$ the Sudakov exponent vanishes, as it should. For the processes considered in this analysis, it is customary to choose the final scales as $\mu_f^2 = \zeta_f = Q^2$ [2], which explains the Q dependence of the structure functions in Eqs. (2) and (8). Given the structure of the evolution equations, it is possible to introduce power corrections to the renormalization group equation for the Collins-Soper kernel K [8]. This results in a non-perturbative correction term, $g_K(\boldsymbol{b}_T^2)$, for which we choose a specific functional form:

$$K(|\boldsymbol{b}_T|, \mu_i) = K(b_{T*}, \mu_i) + g_K(|\boldsymbol{b}_T|), \qquad g_K(\boldsymbol{b}_T^2) = g_2^2 \frac{\boldsymbol{b}_T^2}{4}. \tag{13}$$

In order not to affect the perturbative calculation at small $|\boldsymbol{b}_T|$, the non-perturbative term needs to vanish in the limit $|\boldsymbol{b}_T| \to 0$. The TMD PDF (FF) at the input scales can be factorized on the basis of collinear PDFs (FFs):

$$\tilde{f}_1^a(x, \boldsymbol{b}_T^2; \mu_i, \zeta_i) = \sum_b \int_x^1 \frac{ds}{s} C_{a\leftarrow b}(s, |\boldsymbol{b}_T|; \mu_i, \zeta_i)\, f_1^b\!\left(\frac{x}{s}; \mu_i\right) \equiv [C \otimes f_1](x, |\boldsymbol{b}_T|; \mu_i, \zeta_i), \tag{14}$$

where the sum runs over quarks, antiquarks, and the gluon. Since the matching coefficients C are determined as a perturbative expansion in powers of $\alpha_s(\mu_b)$, Eq. (14) is formally valid only at low $|\boldsymbol{b}_T|$ and we introduce a flavor-independent non-perturbative factor to multiply the matching in Eq. (14). For the TMD PDF it is defined as:

$$f_{1\,NP}(x, \boldsymbol{b}_T^2; Q_0) = \frac{g_1(x)\, e^{-g_1(x)\frac{\boldsymbol{b}_T^2}{4}} + \lambda^2\, g_{1B}^2(x)\left[1 - g_{1B}(x)\frac{\boldsymbol{b}_T^2}{4}\right] e^{-g_{1B}(x)\frac{\boldsymbol{b}_T^2}{4}} + \lambda_2^2\, g_{1C}(x)\, e^{-g_{1C}(x)\frac{\boldsymbol{b}_T^2}{4}}}{g_1(x) + \lambda^2\, g_{1B}^2(x) + \lambda_2^2\, g_{1C}(x)} \left[\frac{\mu_b^2}{Q_0^2}\right]^{-g_K(\boldsymbol{b}_T^2)}, \tag{15}$$

and for the TMD FF, instead, the form is:

$$D_{1\,NP}(z, \boldsymbol{b}_T^2; Q_0) = \frac{g_3(z)\, e^{-g_3(z)\frac{\boldsymbol{b}_T^2}{4z^2}} + \frac{\lambda_F}{z^2}\, g_{3B}^2(z) \left[1 - g_{3B}(z)\frac{\boldsymbol{b}_T^2}{4z^2}\right] e^{-g_{3B}(z)\frac{\boldsymbol{b}_T^2}{4z^2}} + \lambda_{F2}\, g_{3C}(z)\, e^{-g_{3C}(z)\frac{\boldsymbol{b}_T^2}{4z^2}}}{g_3(z) + \frac{\lambda_F}{z^2}\, g_{3B}^2(z) + \lambda_{F2}\, g_{3C}(z)} \left[\frac{\mu_b^2}{Q_0^2}\right]^{-g_K(\boldsymbol{b}_T^2)}. \tag{16}$$

The non-perturbative factors $f_{1\,NP}, D_{1\,NP} \to 1$ for $\boldsymbol{b}_T \to 0$. The g_i functions account for the kinematic dependence of the widths of the distributions:

$$g_{\{1,1B,1C\}}(x) = N_{\{1,1B,1C\}} \frac{x^{\sigma_{\{1,2,3\}}}(1-x)^{\alpha^2_{\{1,2,3\}}}}{\hat{x}^{\sigma_{\{1,2,3\}}}(1-\hat{x})^{\alpha^2_{\{1,2,3\}}}}, \quad g_{\{3,3B,3C\}}(z) = N_{\{3,3B,3C\}} \frac{(z^{\beta_{\{1,2,3\}}} + \delta^2_{\{1,2,3\}})(1-z)^{\gamma^2_{\{1,2,3\}}}}{(\hat{z}^{\beta_{\{1,2,3\}}} + \delta^2_{\{1,2,3\}})(1-\hat{z})^{\gamma^2_{\{1,2,3\}}}}, \tag{17}$$

where $\hat{x} = 0.1$, $\hat{z} = 0.5$, and $Q_0 = 1$ GeV^2.

In total there are 26 free parameters: 1 associated to the non-perturbative part of TMD evolution (Eq. (13)), 11 related to the non-perturbative part of the TMD PDF (Eqs. (15), (17)), 14 for the non-perturbative part of the TMD FF (Eqs. (16), (17)).

Experimental data. This fit of unpolarized TMDs is based on the analysis of the "global" set of the experimental data available to extract unpolarized TMDs, namely Semi-Inclusive DIS, Drell-Yan, and Z-boson production. Data for electron-positron annihilation into two hadrons are not available yet. We do not consider data from processes involving jet-based quantities, such as the thrust, given the significant differences of the involved formalism. We also do not consider data for W-boson production, given its relation with the flavor structure of the TMDs [9], which is beyond the scope of this analysis. In total we analyze 2021 data points, of which 1547 are from SIDIS measured by the Hermes and Compass collaborations. The first provides unpolarized multiplicities for scattering off a proton and deuteron target, with identified positive and negative pions and kaons in the final state. The second provides multiplicities for scattering off a deuteron with identified charged hadrons in the final state. The rest of the data is for Drell-Yan and Z boson production, both in the collider mode (from the ATLAS, CMS, CDF, D0, STAR, PHENIX collaborations) and in the fixed-target mode at low energy (from the E288, E605, E772 collaborations).

Results. This fit is performed at an approximate N^{3}LL perturbative accuracy [7], and we rely on the following choices for the collinear PDFs and FFs: MMHT2014nnlo68cl for the proton quark PDFs (to describe the deuteron we rely on the same set and isospin symmetry), DSS14-NLO for the quark-to-pion FFs, DSS17-NLO for the quark-to-kaon FFs. The lack of an extraction of pion and kaon FFs at NNLO is what prevents us from reaching a complete N^{3}LL accuracy. On top of the experimental uncertainties, we associate a theoretical error to the observables computed in TMD factorization, with two contributions: the first is the hessian error stemming from the aforementioned collinear parton distributions, which we consider fully correlated; the second is an uncorrelated 0.5% error that we include as a conservative estimate of the error arising from scale uncertainties and from the choice of the collinear PDF set.

We implement the following cuts in order to restrict the analysis to the small transverse momentum region (see also Ref. [3] for a similar choice):

$$|\boldsymbol{q}_T|_{\,|\,\mathrm{DY/Z}} < 0.20\, Q\,, \qquad |\boldsymbol{P}_{hT}|_{\,|\,\mathrm{SIDIS}} < \min\left\{z\,Q\,, \min\left[c_1\,Q\,, c_2\,z\,Q\right] + c_3\right\} \mathrm{GeV}\,, \tag{18}$$

where $c_1 = 0.2$, $c_2 = 0.5$, $c_3 = 0.3$. In the SIDIS case, the structure of Eq. (18) guarantees that $|\boldsymbol{q}_T| < Q$, whereas for the Drell-Yan the cut is more stringent. The cut is reduced to 0.18 for the very precise ATLAS data.

With 200 Monte Carlo replicas, 2021 data points, and 26 parameters, we obtain a χ^2/data of 1.063 ± 0.005. In Fig. 1 we provide an example of the extracted TMDs. The plots show the whole distributions, including perturbative and non-perturbative components. The shape of the non-perturbative parts in Eqs. (15) and (16) is crucial for a correct description of the data. In Fig. 1 (b) one can appreciate the contribution of a weighted Gaussian distribution at small transverse momentum. The complete list of results (theory summary, global statistical estimators, the distribution of best fit parameters and their correlations, the χ^2 distribution and the contributions of each dataset to it, the error function distribution, the comparison between theory and experimental data, and the extracted TMDs) obtained from the fit presented in this contribution is available at the following public git repository in the form of a html file:

https://github.com/MapCollaboration/TMDMAP22-results

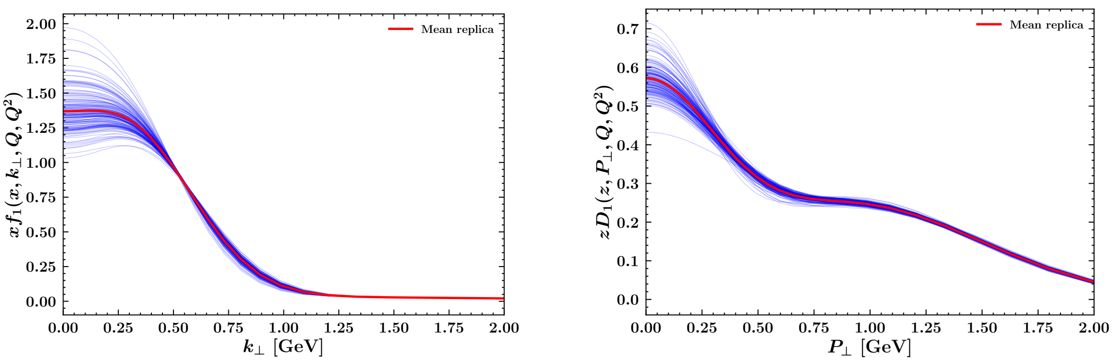

(a) (b)

Fig. 1. (a) TMD PDF for a d quark in a proton at $Q = 2$ GeV and $x = 0.01$; (b) TMD FF for a d quark fragmenting into a π^- at $Q = 2$ GeV and $z = 0.3$. The flavor dependence enters only from the collinear distributions.

Acknowledgments. This work is supported by the European Union's Horizon 2020 programme under grant agreement No. 824093 (STRONG2020). C.B. is supported by the DOE contract DE-AC02-06CH11357. A.S. acknowledges support from the European Commission through the Marie Skłodowska-Curie Action SQuHadron (grant agreement ID: 795475).

References

[1] A. Bacchetta, M. Diehl, K. Goeke, A. Metz, P. J. Mulders and M. Schlegel, JHEP **02**, 093 (2007) doi:10.1088/1126-6708/2007/02/093 [arXiv:hep-ph/0611265 [hep-ph]].
[2] J. Collins, *Foundations of perturbative QCD*, Cambridge University Press (2011).
[3] A. Bacchetta, F. Delcarro, C. Pisano, M. Radici and A. Signori, *JHEP* **1706** (2017) 081 [arXiv:1703.10157 [hep-ph]].
[4] I. Scimemi and A. Vladimirov, JHEP **06**, 137 (2020) doi:10.1007/JHEP06(2020)137 [arXiv:1912.06532 [hep-ph]].
[5] J. Osvaldo Gonzalez-Hernandez, PoS **DIS2019**, 176 (2019) doi:10.22323/1.352.0176
[6] F. Piacenza, Ph.D. thesis, U. of Pavia, 2020.
[7] A. Bacchetta, V. Bertone, C. Bissolotti, G. Bozzi, F. Delcarro, F. Piacenza and M. Radici, JHEP **07**, 117 (2020) doi:10.1007/JHEP07(2020)117 [arXiv:1912.07550 [hep-ph]].
[8] M. Grewal, Z. B. Kang, J. W. Qiu and A. Signori, Phys. Rev. D **101**, no.11, 114023 (2020) doi:10.1103/PhysRevD.101.114023 [arXiv:2003.07453 [hep-ph]].
[9] A. Bacchetta, G. Bozzi, M. Radici, M. Ritzmann and A. Signori, Phys. Lett. B **788**, 542-545 (2019) doi:10.1016/j.physletb.2018.11.002 [arXiv:1807.02101 [hep-ph]].